Mathematical Malaria Model

Roshan Kern

May 1st, 2023

The paper we are recreating: *A Mathematical Model for the Dynamics and Control of Malaria in Nigeria* by O.C. Collins and K.J. Duffy.

Introduction

Background and Hypothesis

The paper A Mathematical Model for the Dynamics and Control of Malaria in Nigeria by O.C. Collins and K.J. Duffy takes a mathematical modeling approach to understanding and predicting the dynamics of malaria in Nigeria. Mathematical models can be used with actual disease data to create parameters allowing the model to resemble the original data (Collins & Duffy, 2022). For example, Oguntolu et al. used actual Nigerian measles data to fit a mathematical model and its parameters to follow the measles disease dynamics (Olumuyiwa et al., 2022). These mathematical models can then be used to project the dynamics of the disease across a population (Collins & Duffy, 2022). For example, Khan et al. present a mathematical model for predicting the spread of COVID-19 in India (Kumar et al., 2021). In the paper we are attempting to replicate, the authors derive a mathematical model of the spread of malaria in Nigeria, fit the model to real data, and predict the spread of the disease over the next 50 years. The authors select various variables to measure and implement in their model for their analysis. These include susceptible humans, populations of humans infected with resistant/sensitive strains, treated individuals with resistant/sensitive strains, recovered/immune humans, susceptible mosquitoes, and a population of infected mosquitoes (Collins & Duffy, 2022). The authors design the model with 14 parameters related to the spread of malaria disease through mosquito and human populations (Collins & Duffy, 2022). Similar to Hengki Tasman and Fatmawati, the authors investigate the effect of varying control parameters on the pervasiveness of the disease (Fatmawati, & Tasman, 2015). The paper hypothesizes that a model can be used to indicate that the prevalence of malaria in Nigeria will decrease if control measures, particularly improved treatment and increased mosquito net usage, are improved and made widespread.

Significance

Despite the advances in modern medicine, malaria still has a significant prevalence throughout the world. In 2015, there were an estimated 214 million malaria cases worldwide, 438,000 of these resulting in death (Basu et al., 2017). Malaria is caused by one of many plasmodium species capable of causing life-threatening multi-organ disease (Lalloo et al., 2016). This parasite has a life cycle that takes place in both humans and mosquitoes. In other

words, the plasmodium infects both human and mosquito populations (Milner, 2018). The analysis done by O.C. Collins and K.J. Duffy indicates that without any changes in control parameters, malaria will likely remain endemic in Nigeria in the next 50 years. However, improving control measures (specifically on the resistant strain), improving treatment, and increasing mosquito nets' use can dramatically decrease malaria in Nigeria in the future (Collins & Duffy, 2022). This paper, in particular, utilizes drug-resistant control measures with actual malaria data to fit and make predictions with the model, which the authors claim no other papers have done. In the larger biological and social context, confirming the hypothesis of this paper would indicate which control measures should be increased best to reduce the future prevalence of malaria in Nigeria.

Extension

Genetically modified mosquitoes have been shown to stunt malaria growth in mosquitoes (Pascini et al., 2022). Although many methods exist to introduce a malaria-stunting gene to a mosquito population, the authors identify Medea as the most viable current method. In Medea, all mosquito children that do not inherit the Medea allele will die. Thus, mosquitoes that inherit this modified allele from their parents will have an advantage over their siblings that did not inherit the desired gene (Marshall & Taylor, 2009). To create a simple model of a malaria-stunting Madea gene spreading through a population, we can assume that the gene spreads through the mosquito population like a disease. Reducing the parameter for human-to-mosquito transmission in the original model can represent the effect of the malaria-stunting gene. Examining a model that incorporates a reduction factor resulting from the spread of a malaria-stunting gene in the mosquito population of Nigeria would illustrate how malaria prevalence would decrease under these conditions. Furthermore, studying this extended model would provide an idea of what efficacy and transmission rate for the malaria-stunting gene are necessary to decrease malaria's future prevalence in Nigeria significantly. From the biological context, this would give scientists an estimate of how efficacious and transmissible this engineered gene would need to be before it should be released.

Model Description

State Variables and Parameters

Table 1: State Variables (Nondimensionalized Model 2)

Variable	**Description**	**Initial Value**	**Initial Value Source**
s(t)	Normalized susceptible humans at time	0.56	Figure 4 Plot 1
$i_r(t)$	Normalized population of humans infected with resistant strains at time t	0.22	Figure 4 Plot 2
$i_s(t)$	Normalized population of humans infected with sensitive strains at time t	0.22	Figure 4 Plot 2
$t_r(t)$	Normalized treated individuals with resistant strains at time t	0	Human Vars (s-r) sum to 0
$t_s(t)$	Normalized treated individuals with sensitive strains at time t	0	Human Vars (s-r) sum to 0
r(t)	Normalized recovered/immune humans at time t	0	Human Vars (s-r) sum to 1
x(t)	Normalized susceptible mosquitoes at time t	?	Need to find with manipulate
y(t)	Normalized population of infected mosquitos at time t	$1-x_0$	x(t) and y(t) should sum to 1

Table 2: Parameters (Nondimensionalized Model 2)

Parameter	**Description**	**Value**	**Source**
β **	Infection rate from mosquitoes to human	0.0044	Literature
α_r	Infection rate from $I_r(t)$ to mosquitoes	0.0044	Literature

α_s	Infection rate from $I_s(t)$ to mosquitoes	0.0044	Literature
μ	Natural birth/mortality rate of humans	$\frac{1}{70*365}$	Literature
ρ *	Fraction of humans infected with drug resistant strains	0.3	Literature
c *	Reduction of infection rate due to use of mosquitoes nets	0.1742	Model Fit
σ_r	Treatment rate of $I_r(t)$	0.0024	Model Fit
σ_s	Treatment rate of $I_s(t)$	0.0027	Model Fit
γ_r	Expected recovery rate of $T_r(t)$	0.00019	Literature
γ_s	Expected recovery rate of $T_s(t)$	0.0022	Literature
ε_r	Rate of treatment failure for $T_r(t)$	0.0055	Model Fit
ε_s	Rate of treatment failure for $T_s(t)$	0.0006	Model Fit
ω	Waning immunity rate of $R(t)$	0.005	Literature
ξ	Natural birth/death rate of mosquitoes	$\frac{1}{15}$	Literature
m *	Average number of mosquitoes per human	10	Email with authors

Note: All parameters have unit of day^{-1} except those marked with *, which are dimensionless. Parameters with a unit of day^{-1} are converted to a unit of year^{-1} to suit the time scale of the study (Collins & Duffy, 2022)

** The transmission rate β is multiplied by a seasonality factor $(1+\cos(\pi t/15))$ to account for irregular seasonal patterns in the data (Collins & Duffy, 2022).

Model Assumptions

Collins and Duffy (2022) describe the following assumptions for the model of malaria dynamics in Nigeria:

- All humans can be put into one of the following categories (encompassed by the first 6 state variables): susceptible, infected with resistant strain, infected with sensitive strain, treated with resistant strain, treated with susceptible strain, recovered/immune.
- All mosquitoes can be put into one of the following categories (encompassed by the last 2 state variables): susceptible, infected.
- The birth and death rates for mosquito and human populations are the same, thus these total populations remain constant.
- Humans recovering from malaria have temporary immunity from reinfection (and belong in the recovered/immune category).

Model Equations

The equations used to describe the dynamics of malaria in Nigeria are described below. These equations comprise Model 1 from the paper. Collins and Duffy (2022) illustrate the malaria model with the schematic below:

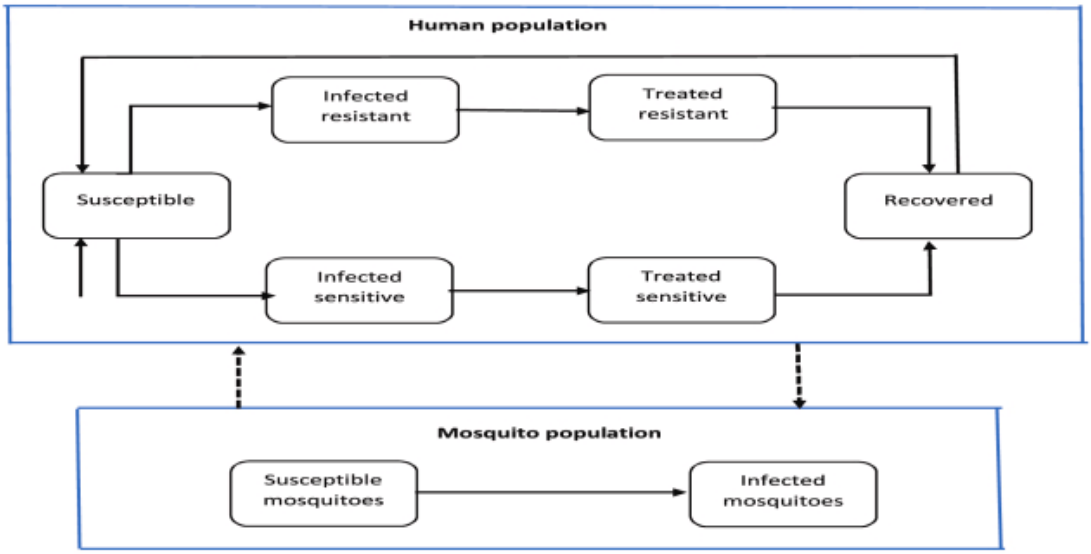

Figure 1. Schematic illustration of the malaria model (Collins & Duffy, 2022).

Equation 1:

$$\frac{dS(t)}{dt} = \mu N_h(t) - \frac{(1-c)m\beta S(t)Y(t)}{N_v(t)} - \mu S(t) + \omega R(t)$$

This is the expression for the change in the susceptible human population. The first component represents humans being born (human birth rate * total human population); these

humans are susceptible because they are assumed to be born without malaria. The second component represents humans being infected which are subtracted from the susceptible human population; (1-c) represents the chance that a mosquito net is not being used (use would prevent infection), $\frac{m*S(t)*Y(t)}{N_v(t)}$ represents the number of susceptible human and infected mosquito interactions (average number of mosquitoes/human * number of susceptible humans * proportion of mosquitoes that are infected), β represents the transmission rate which is obviously proportional to mosquito to human infection. The third component represents natural deaths of susceptible humans which are removed from the susceptible human population (natural death rate of humans * susceptible human population). The final component represents recovered/immune humans that lose their immunity and rejoin the susceptible population (waning immunity rate * recovered human population).

Equation 2:

$$\frac{dI_r(t)}{dt} = \frac{\rho(1-c)m\beta S(t)Y(t)}{N_v(t)} - (\sigma_r + \mu)\, I_r\,(t) + \epsilon_r T_r\,(t)$$

This is the expression for the change in the population of humans infected with the resistant strain. The first component represents susceptible human infection with the resistant strain; this component is very similar to the second component from equation 1, with the addition of the entire component being multiplied by the fraction of humans infected with the resistant strain (ρ). Thus, this first component represents newly humans infected * fraction of humans infected with the resistant strain. The second component represents the humans leaving the resistant infection population because they are treated (multiplication of resistant treatment rate σ_r) or because they die with the natural death rate (multiplication of natural death rate μ). The final component represents treated humans with the resistant strain joining the infected population as their treatment fails, hence the treatment failure rate (ϵ_r) is multiplied by the population of humans being treated for the resistant strain.

Equation 3:

$$\frac{dI_s(t)}{dt} = \frac{(1-\rho)(1-c)m\beta S(t)Y(t)}{N_v(t)} - (\sigma_s + \mu)\, I_s\,(t) + \epsilon_s T_s\,(t)$$

This is the expression for the change in the population of humans infected with the sensitive strain. It nearly exactly resembles equation 2 with two changes. 1) Parameters and state variables related to the resistant strain are changed to be related to the sensitive strain as

we are now trying to find the change in the human population infected with the sensitive strain. 2) In component 1, the fraction of humans infected with the resistant strain (ρ) is replaced by (1-ρ), which represents the fraction of humans infected with the sensitive strain (these two fractions must add to 1 as only two strains exist in this model).

Equation 4:

$$\frac{dT_r(t)}{dt} = \sigma_r I_r(t) - (\gamma_r + \epsilon_r + \mu) T_r(t)$$

This is the expression for the change in the population of humans being treated for their resistant strain infection. The first component represents humans infected with the resistant strain becoming treated, hence the population of humans infected with the resistant strain ($i_r(t)$) is multiplied by the resistant strain treatment rate (σ_r). The second component represents a decrease in the population of humans being treated for the resistant strain due to treatment succeeding and the humans recovering and becoming immune (γ_r), the treatment failing and the humans returning to infected (ϵ_r), or the treated humans dying at their normal rate (μ).

Equation 5:

$$\frac{dT_s(t)}{dt} = \sigma_s I_s(t) - (\gamma_s + \epsilon_s + \mu) T_s(t)$$

This is the expression for the change in the population of humans being treated for their sensitive strain infection. It is nearly the exact same as equation 5, with all the parameters and state variables related to the resistant strain are changed to be related to the sensitive strain.

Equation 6:

$$\frac{dR(t)}{dt} = \gamma_r T_r(t) + \gamma_s T_s(t) - (\omega + \mu) R(t)$$

This is the expression for the change in the population of humans recently recovered and temporarily immune. The first component represents humans successfully treated for a resistant strain infection, hence the rate of resistant treatment success (γ_r) is multiplied by the population of humans being treated for the resistant strain infection ($T_r(t)$). Similarly, the second component represents humans successfully treated for a sensitive strain infection, hence the rate of sensitive treatment success (γ_s) is multiplied by the population of humans being treated for the sensitive strain infection ($T_s(t)$). The final component represents humans being removed from the recovered/immune population (R(t)) because they either lose their immunity (hence

multiplication by waning immunity rate ω) or they die as they naturally would (hence multiplication by natural death rate μ).

Equation 7:

$$\frac{dX(t)}{dt} = \xi N_v(t) - \frac{(1-c)\alpha_r X(t) I_r(t)}{N_h(t)} - \frac{(1-c)\alpha_s X(t) I_s(t)}{N_h(t)} - \xi X(t)$$

This is the expression for the change in the population of mosquitoes susceptible to malaria-parasite infection. The first component represents the addition of mosquitoes to this population as mosquitoes are born (mosquitoes are born susceptible), hence the natural birth rate (ξ) is multiplied by the total mosquito population ($N_v(t)$). The second and third components represent susceptible mosquitoes becoming infected with the resistant and sensitive strains respectively (and thus leaving the susceptible population). For each of these components, the chance of infection after mosquito net use (1-c) is multiplied by the infection rate from humans infected with the respective strain to mosquitoes (*α*), the population of humans infected by the respective strain (I(t)), and the proportion of mosquitoes susceptible to infection ($\frac{X(t)}{N_h(t)}$). The final component represents susceptible mosquitoes naturally dying, hence the natural death rate (ξ) is multiplied by the total mosquito population (X(t)).

Equation 8:

$$\frac{dY(t)}{dt} = \frac{(1-c)\alpha_r X(t) I_r(t)}{N_h(t)} + \frac{(1-c)\alpha_s X(t) I_s(t)}{N_h(t)} - \xi Y(t)$$

This is the expression for the change in the population of mosquitoes infected with the mosquito parasite. The first two components are the opposite of the second and third components from equation 7 as these newly-infected mosquitoes are added to the infected mosquito population. The final component represents infected mosquitoes naturally dying, hence the natural death rate (ξ) is multiplied by the total mosquito population (X(t)).

Nondimensionalization

Collins and Duffy (2022) normalize model 1 (described with the equations above) to remove the units of humans and mosquitoes from their respective state variables. To remove these units, the state variables are normalized by the total population of humans ($N_h(t)$) or the total population of mosquitoes ($N_v(t)$) where appropriate (Collins & Duffy, 2022). This normalization results in the equations below that comprise the nondimensionalized model 2.

Human state variables scaled by total human population $N_h(t)$:

$$s(t) = \frac{S(t)}{N_h(t)}, \quad i_r(t) = \frac{I_r(t)}{N_h(t)}, \quad i_s(t) = \frac{I_s(t)}{N_h(t)}, \quad \tau_r(t) = \frac{T_r(t)}{N_h(t)}, \quad \tau_s(t) = \frac{T_s(t)}{N_h(t)}, \quad r(t) = \frac{R(t)}{N_h(t)},$$

Mosquito state variables scaled by total mosquito population $N_v(t)$:

$$x(t) = \frac{X(t)}{N_v(t)}, \quad y(t) = \frac{Y(t)}{N_v(t)}$$

These scaled variables can be used to rewrite model 1 as model 2, which is described with the equations below:

$$\begin{aligned}
\frac{ds(t)}{dt} &= \mu - (1-c)\, m\beta s(t)\, y(t) - \mu s(t) + \omega r(t), \\
\frac{di_r(t)}{dt} &= \rho(1-c)\, m\beta s(t)\, y(t) - (\sigma_r + \mu)\, i_r(t) + \epsilon_r \tau_r(t), \\
\frac{di_s(t)}{dt} &= (1-\rho)(1-c)\, m\beta s(t)\, y(t) - (\sigma_s + \mu)\, i_s(t) + \epsilon_s \tau_s(t), \\
\frac{d\tau_r(t)}{dt} &= \sigma_r i_r(t) - (\gamma_r + \epsilon_r + \mu)\, \tau_r(t), \\
\frac{d\tau_s(t)}{dt} &= \sigma_s i_s(t) - (\gamma_s + \epsilon_s + \mu)\, \tau_s(t), \\
\frac{dr(t)}{dt} &= \gamma_r \tau_r(t) + \gamma_s \tau_s(t) - (\omega + \mu)\, r(t), \\
\frac{dx(t)}{dt} &= \xi - (1-c)\, \alpha_r x(t)\, i_r(t) - (1-c)\, \alpha_s x(t)\, i_s(t) - \xi x(t), \\
\frac{dy(t)}{dt} &= (1-c)\, \alpha_r x(t)\, i_r(t) + (1-c)\, \alpha_s x(t)\, i_s(t) - \xi y(t).
\end{aligned} \tag{2}$$

Simulation Mechanisms

Because we have a system of differential equations with 8 state variables, we can solve this system in Mathematica with the initial values of each of the 8 state variables. We are able to derive the first 6 state variables' initial values by looking at the plots in Figure 4. However, we still do not know the initial values of the last 2 state variables x(t) and y(t). Thus, it is necessary to use a Manipulate function in Mathematica to find the values of x_0 and y_0 that will recreate Figure 3. Given that x(t) and y(t) should sum to 1 (they comprise the normalized mosquito population), we only need to manipulate one slider and should be able to quickly find x_0 and y_0.

With the definitions and initial values of the 8 state variables, we will use Mathematica's NDSolve function to perform numerical integration and derive an interpolation function for the 8

state variables over various times. For Figure 3, we will derive an interpolation function for $i_r(t)+i_s(t)$ from t=0 to t=18. For Figure 4, we will derive an interpolation function for s(t), $i_r(t)$ and $i_s(t)$ (plotted separately), and $i_r(t)+i_s(t)$ from t=0 to t=50 years.

Figures 5-7 detail the effects of changing various control parameters. The incidence of the susceptible and resistant strains at t=50 (2050) are plotted against the values of the various control parameters: treatment rates, treatment failures, and the use of mosquito nets. To create these plots with Mathematica, we will create a function to derive the incidence of the susceptible and resistant strains at t=50 (2050) with a particular value for the control parameters. This function will then be evaluated over the range given for each control parameter in Figures 5-7.

We will also attempt to reproduce Figures 8 and 9 which show the sensitivity indices for basic reproduction number (R_0) and coexistence endemic equilibrium (COE) respectively. Collins and Duffy (2022) perform sensitivity analysis to determine which parameters have a significant effect on R_0, which represents the expected number of cases one person infected with malaria can be expected to generate in a population of all susceptible people. Similarly, COE gives an idea of the future endemic equilibrium, where lower numbers indicate less chance of an endemic equilibrium. To get sensitivity indices for both of these values, we will create a function that adjusts each parameter value and recalculates R_0/COE, and then derives the sensitivity indices from these recalculated values. We will need to use Mathematica's BarChart function to replicate Figures 8 and 9 with the derived sensitivity indices.

Extension

As mentioned earlier, we will extend this model by simulating the spread of a malaria-stunting gene through the mosquito population. To represent the effect of the malaria-stunting gene on parasite transmission, we will multiply the parameters for mosquito infection (α_r, α_s) by a "reduction factor" that models both the spread of the gene through the population and the gene's efficacy in reducing malaria growth in a mosquito.

We can model the spread of a malaria-stunting gene through a mosquito population the same way we would model the spread of a disease. Collins and Abdelal (2018) describe the simplest model for population infection as the SI model (susceptible and infected). In this model, the infected population can be represented as a function of time:

$$i(t) = \frac{i_0 e^{\beta t}}{1 - i_0 + i_0 e^{\beta t}}.$$

where i_0 is percent of population infected at t=0 and β is transmission rate.

We repurpose this model to define the reduction factor as a function of time with parameters pr (parasite reduction) and sc (spread constant). Parasite reduction represents the chance that the malaria-stunting gene successfully prevents malaria (ex pr=0.9 would represent a gene that successfully stunts malaria growth 90% of the time). Spread constant encompasses the speed with which the malaria-stunting gene spreads through the mosquito population. Wade and Beeman (1994) describe that for the gene drive method we are modeling in this extension (Medea), the spread rate strongly depends on its release ratio. Thus, the spread constant includes both the rate of spread and release ratio of genetically-modified mosquitoes.

Our reduction factor is defined as

$$rf = 1 - pr \frac{e^{sc\,t}\,sc}{1-sc+e^{sc\,t}\,sc}$$

Here, we calculate 1-i(t) described above because we want the chance that a mosquito can grow the malaria parasite (and thus is not "infected" by the malaria-stunting gene). We also multiply i(t) by the parasite reduction (pr) parameter to account for the fact that some mosquitoes with the malaria-stunting gene may still grow the parasite. We also choose to implement this reduction factor after 2025 as this would be a reasonable time for genetically-modified mosquitoes to be released in Nigeria. Thus, we use the state variable values at t=25 years (2025) from the original model as the initial values for the extended model.

Results

Figure 2

Original Results

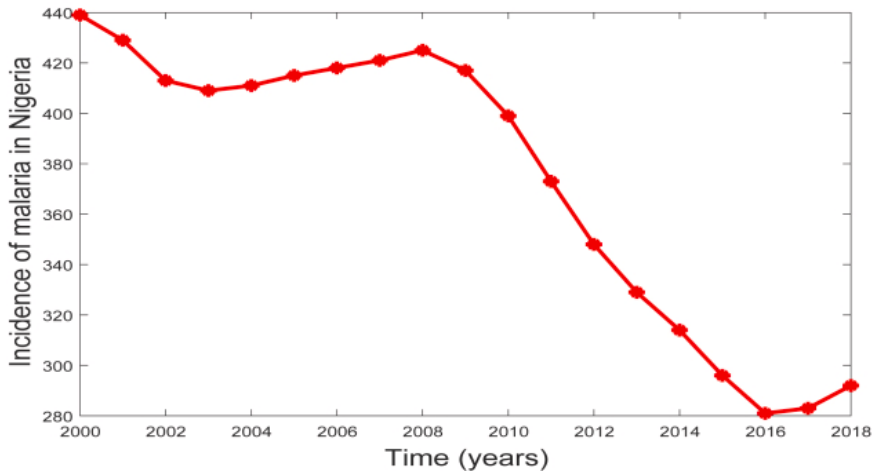

Figure 2. Plot showing the incidence of malaria per 1000 population at risk in Nigeria from 2000 to 2018 (The World Bank, 2021).

Our Results

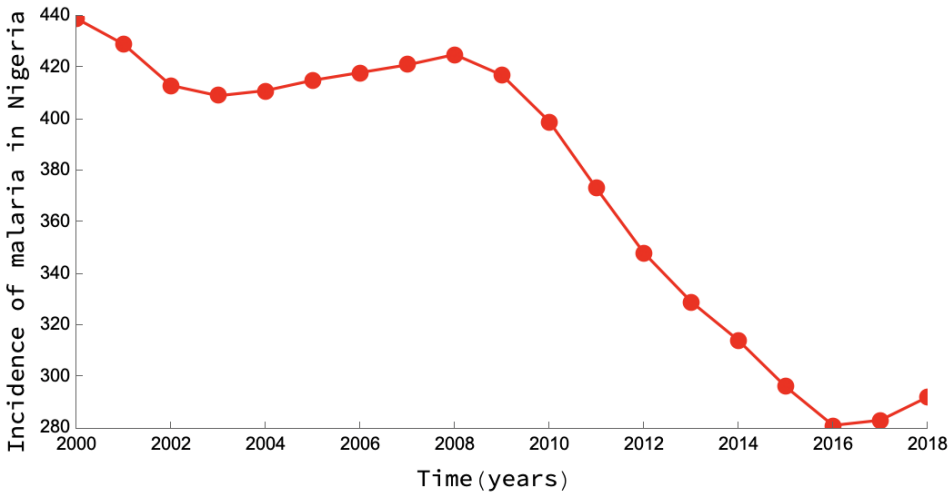

Figure 2. Incidence per 1000 population at risk in Nigeria from 2000 to 2018 as per The World Bank (2021).

Figure 2 illustrates the historical incidence of malaria in Nigeria over 2000-2018 per 1000 population at risk. Collins and Duffy (2022) retrieved this historical data from The World Bank

(2021), which has since been updated and thus has different incidence data. After emailing the original authors, Collins and Duffy kindly shared the original data they used during their model construction.

From these results, one might conclude that malaria's incidence and subsequent dangers are on a steep decline in Nigeria and will continue along this path. However, this is a dangerous assumption to make solely from the historical incidence of a disease. A model of the dynamics of malaria can give us better insight into how the virus might progress in Nigeria.

Figure 3

Original Results	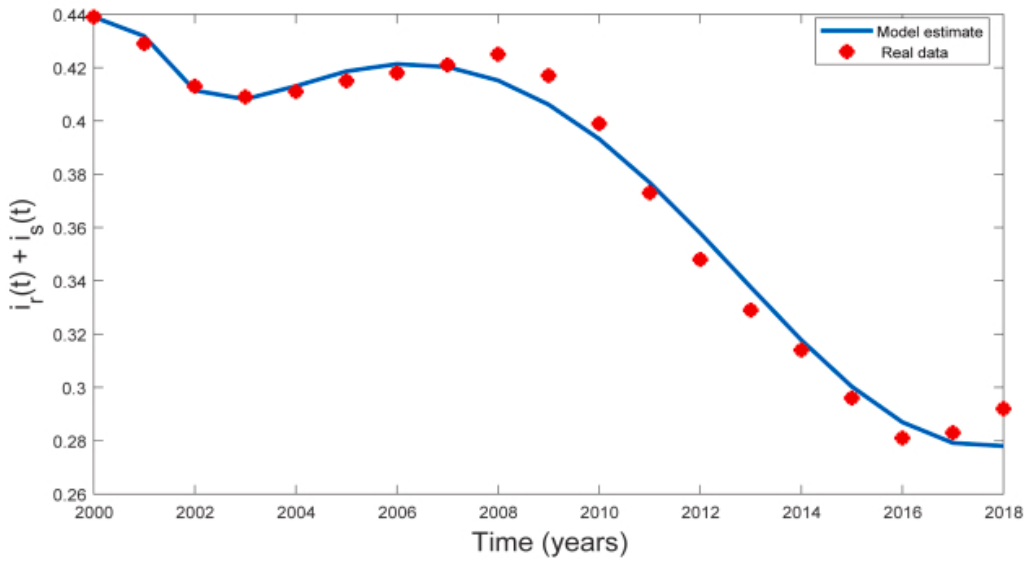

Figure 3. Model fit of the proportion of incidence of malaria per 1000 population at risk in Nigeria from 2000 to 2018, where blue lines represent the model fit and circles mark the confirmed cases.

Our Results	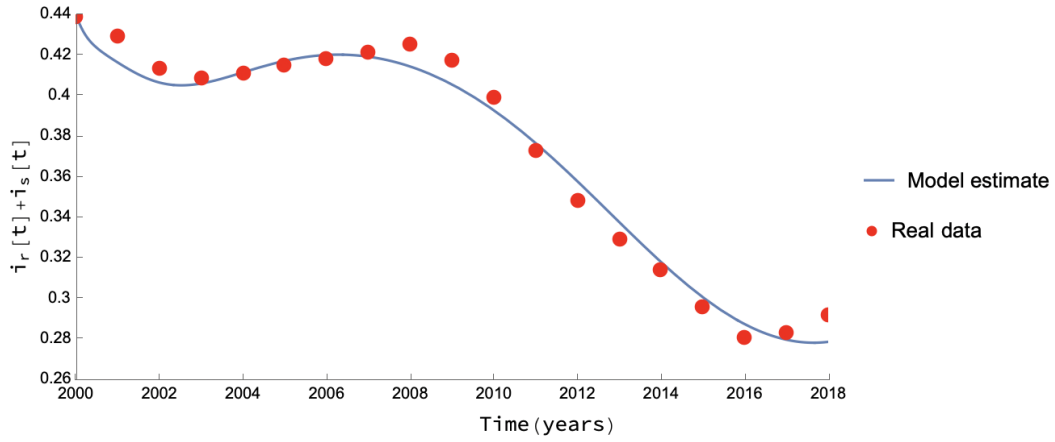

Figure 3. Model estimate (after parameter and initial value fit) vs real data for incidence of malaria in Nigeria from 2000 to 2018.

Figure 3 illustrates the sum of the solutions for humans infected with resistant and sensitive strains from 2000 to 2018. For our model, 2000 corresponds to t=0, e.g., t=year-2000. Because the analyzed model is dimensionless (see model description for the creation of the nondimensionalized model), ir(t)+is(t) represents the normalized population of humans infected with resistant and sensitive strains. In other words, ir(t)+is(t) represents the incidence of malaria per 1000 population at risk as a percentage of the total human population. Similarly, the historical incidence data from Figure 2 is normalized to the total human population.

Because we could not discern x(0) or y(0) from the original paper, it was necessary to try and find these values with Manipulate. The figure above is closest to the original, with a fit of x(0) = 0.975. We know 1-x(0) = y(0) because x(t) and y(t) should always add to 1 (they comprise the normalized mosquito population). Thus, y(0) = 0.025.

These results indicate that the model is a good fit for historical malaria incidence in Nigeria. This relatively good fit gives us more confidence in the model's future predictions. When we later use this model to indicate that the prevalence of malaria in Nigeria will decrease if control measures are improved and made widespread, we can be confident that the model used to come to this conclusion can accurately represent real data.

Figure 4

Original Results	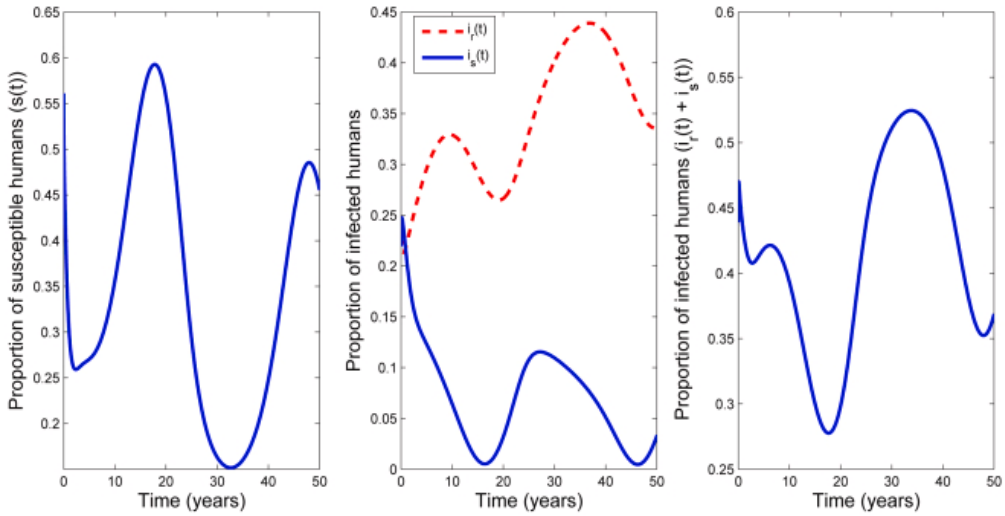

Figure 4. Plot showing the possible long term dynamics of malaria in Nigeria using the estimated parameter values.

Our Results	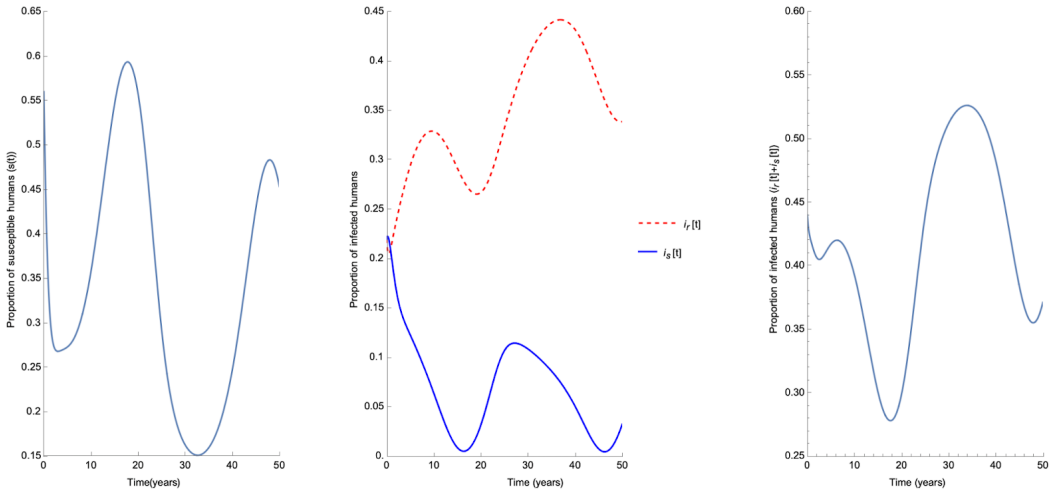

Figure 4. Plot showing the long term dynamics of malaria (2000-2050) in Nigeria as predicted by the fit model. Plot 1 shows the normalized susceptible human population. Plot 2 shows the proportion of infected humans with resistant (red, dashed) and sensitive (blue, solid) strains. Plot 3 shows the total proportion of infected humans.

Figure 4 illustrates the course of malaria in Nigeria from t=0 (2000) to t=50 (2050), as

predicted by the model. Plot 1 (left) illustrates the predicted course of the susceptible human population for 2000-2050. Plot 2 (middle) demonstrates the proportion of humans infected with the resistant strain (red, dashed) or sensitive strain (solid, blue). Plot 3 (right) illustrates the proportion of humans infected with either strain of malaria to give an idea of the total malaria incidence in Nigeria.

These results demonstrate that the decrease in incidence from 2000 to 2020 (see Figure 2) is not indicative of the long-term dynamics of malaria, at least by the model's prediction. On the contrary, the model predicts malaria will likely remain endemic in Nigeria until 2050. Additionally, the resistant strain will drive the malaria outbreak, as shown in plot 2 (middle) by the resistant strain's dominance over the sensitive strain. The hypothesis that increasing control measures can decrease the future prevalence of malaria is essential because, as we can tell from these plots, malaria will remain endemic in Nigeria (by 2050, over 35% of humans have the resistant strain of malaria).

Figure 5

Original Results	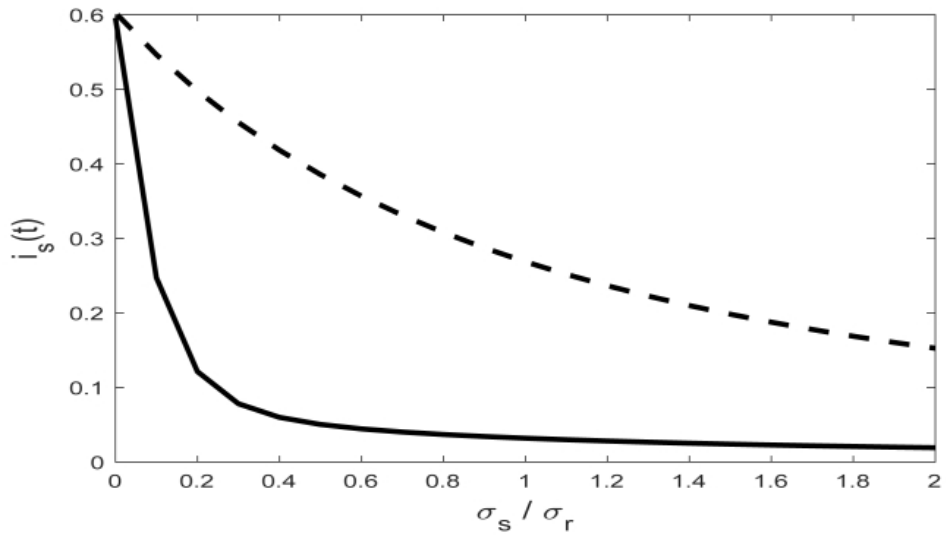

Figure 5. Plot showing the effects of treatment rates (σ_r, σ_s) on the dynamics of infected humans with the resistant strain (dashed line) and the sensitive strain (solid line).

Our Results	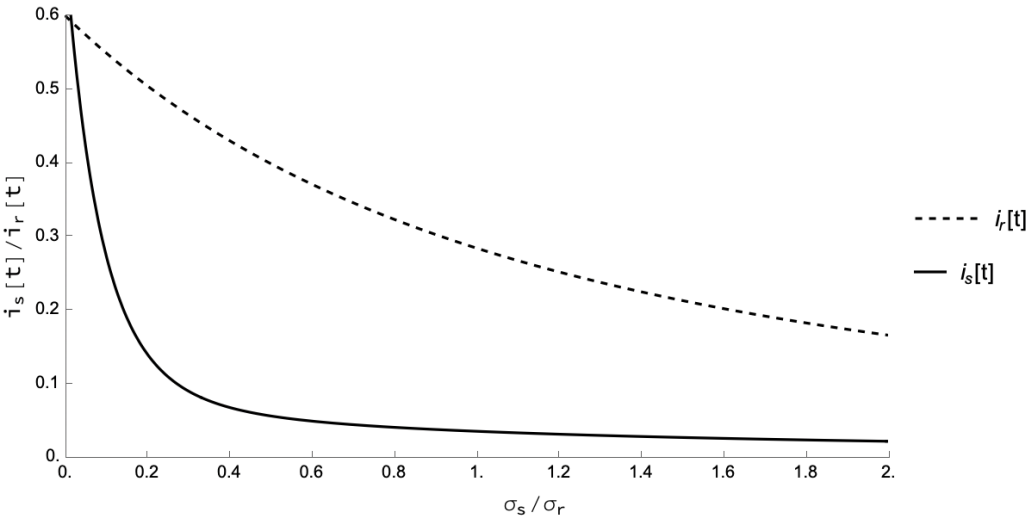

Figure 5. Plot showing $i_r[22]$ and $i_s[50]$ as σ_r and σ_s are increased from 0% to 200% of their original values respectively. All other parameters are kept at their model fit values.

Figure 5 illustrates the effect of varying the treatment rates on the long-term malaria dynamics in Nigeria. The dotted line is produced by multiplying the fit resistant treatment rate (σ_r) by a multiplier between 0 and 2 (x-axis) and finding the normalized population of humans infected with the resistant strain ($i_r(t)$) at a specific time. Similarly, the solid line is produced by multiplying the fit sensitive treatment rate (σ_s) by a multiplier between 0 and 2 (x-axis) and finding the normalized population of humans infected with the sensitive strain ($i_s(t)$) at a specific time. We varied these specific times to produce a figure as close as possible to the original (see discrepancies below for more information).

These results show how changing the sensitive and resistant treatment rates affect their respective incidences. The dashed line shows that as the resistant treatment rate is increased to double its fit value, the normalized population of humans with the resistant strain at the specific time decreases to around 0.15. The solid line shows that as the sensitivity treatment rate is increased to double its fit value, the normalized population of humans with the sensitive strain at the specific time decreases to close to 0. Thus, this figure supports the hypothesis that increasing treatment rates will decrease the future prevalence of malaria in Nigeria, especially for the sensitive strain.

Figure 6

Original Results	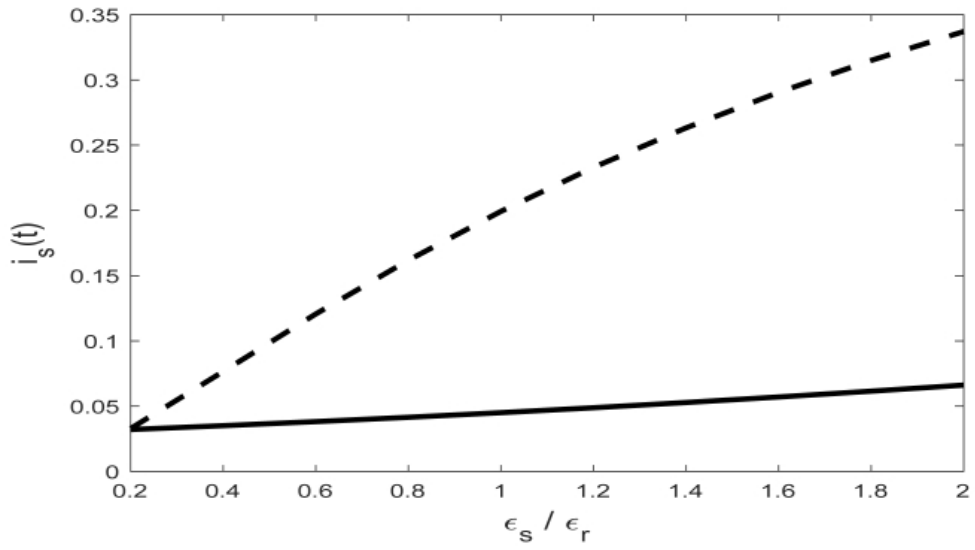

Figure 6. Plot showing the effects of treatment failure (ϵ_r, ϵ_s) on the dynamics of infected humans with the resistant strain (dashed line) and the sensitive strain (solid line).

Our Results	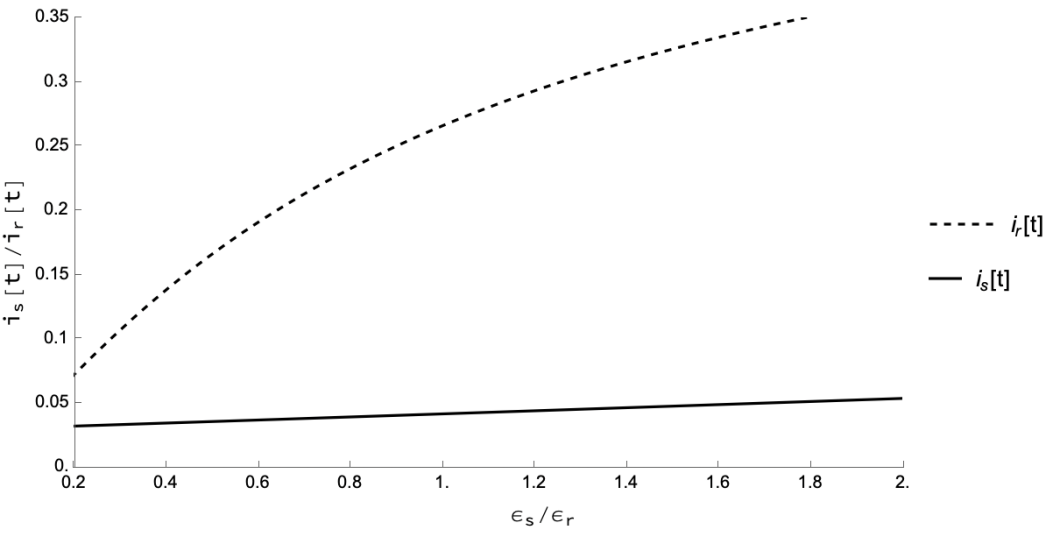

Figure 6. Plot showing $i_r[19]$ and $i_s[41]$ as ϵ_r and ϵ_s are increased from 20% to 200% of their original values respectively. All other parameters are kept at their model fit values.

Figure 6 illustrates the effect of varying the treatment failure rates on the long-term malaria dynamics in Nigeria. The dotted line is produced by multiplying the fit resistant treatment failure rate (ϵ_r) by a multiplier between 0.2 and 2 (x-axis) and finding the normalized population of humans infected with the resistant strain ($i_r(t)$) at a specific time. Similarly, the solid line is produced by multiplying the fit sensitive treatment failure rate (ϵ_s) by a multiplier between 0.2 and 2 (x-axis) and finding the normalized population of humans infected with the sensitive strain ($i_s(t)$) at a specific time. We varied these specific times to produce a figure as close as possible to the original (see discrepancies below for more information).

These results show how changing the sensitive and resistant treatment failure rates affect their respective incidences. The dashed/solid lines show that as the resistant/sensitive treatment failure rates are decreased to 20% of their fit values, the normalized population of humans infected with both strains decreases drastically. This supports the hypothesis that decreasing treatment failure rates will decrease the future prevalence of malaria in Nigeria.

Figure 7

Original Results	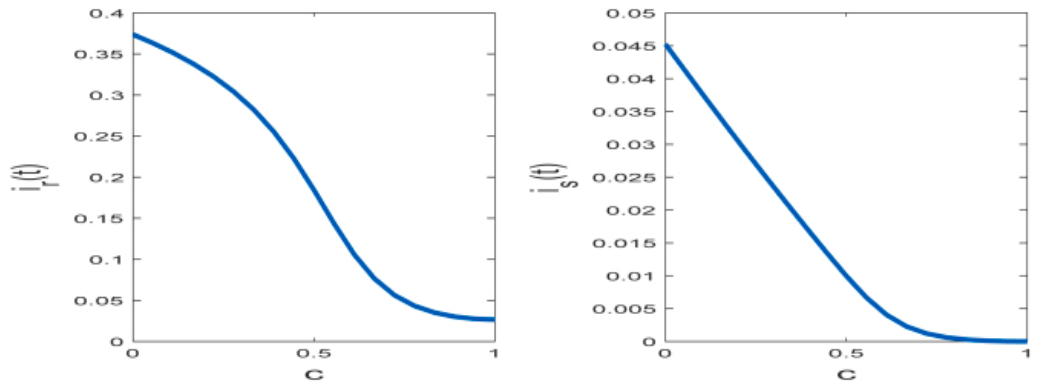

Figure 7. Plot showing the effects of use of mosquitoes net (c) on the dynamics of infected humans with resistant strain and sensitive strain.

Our Results	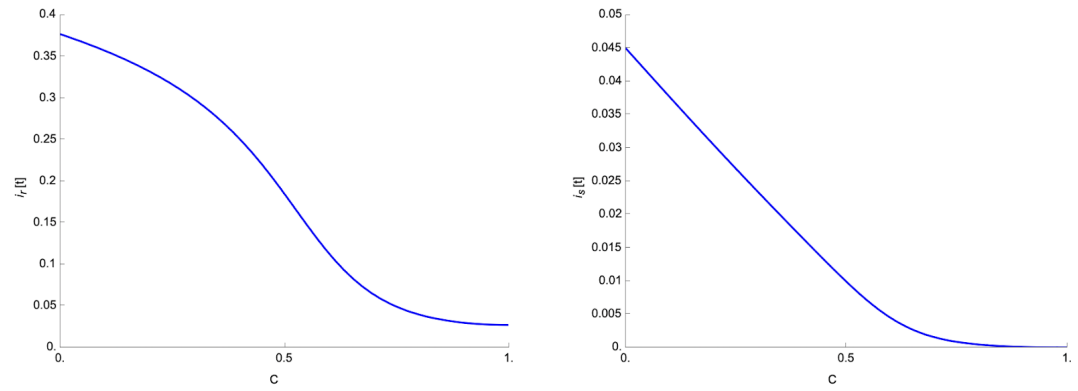

Figure 7. Plot showing $i_r[50]$ and $i_s[50]$ as c is increased from 0 to 1. All other parameters are kept at their model fit values.

Figure 7 illustrates the effects of varying the infection rate reduction due to mosquito nets' use on Nigeria's long-term malaria dynamics. Plot 1 (left) is produced by plotting the normalized population of humans with the resistant strain at time t=50 years given a model with values of c between 0 and 1. Similarly, plot 2 (right) is produced by plotting the normalized population of humans with the sensitive strain at time t=50 years given a model with values of c between 0 and 1.

Clearly, increased use of mosquito nets results in what Collins and Duffy (2022) call a “considerable decreased of the incidence of malaria in Nigeria.” Although the resistant strain is not completely eradicated for higher levels of c, it is reduced to a very low level. This supports the hypothesis that increasing mosquito net use will significantly decrease the future prevalence of malaria in Nigeria.

Figure 8

Original Results	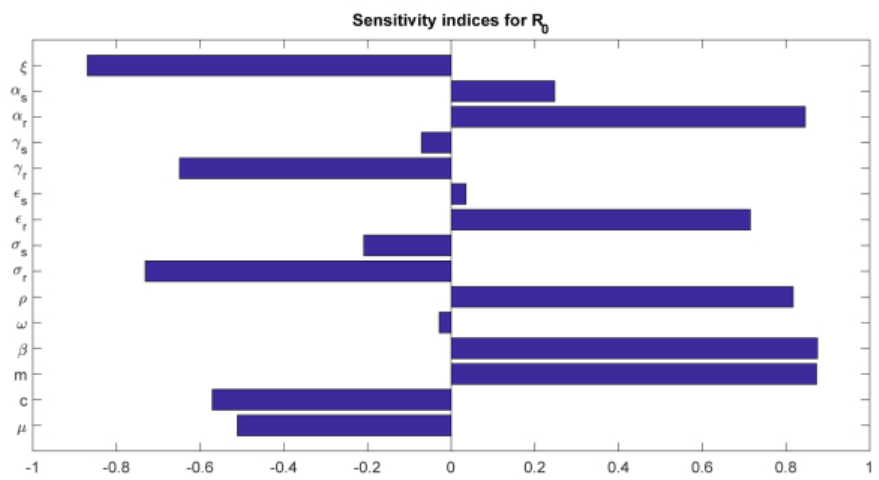

Figure 8. Tornado plot showing the sensitivity indices for R_0.

Our Results	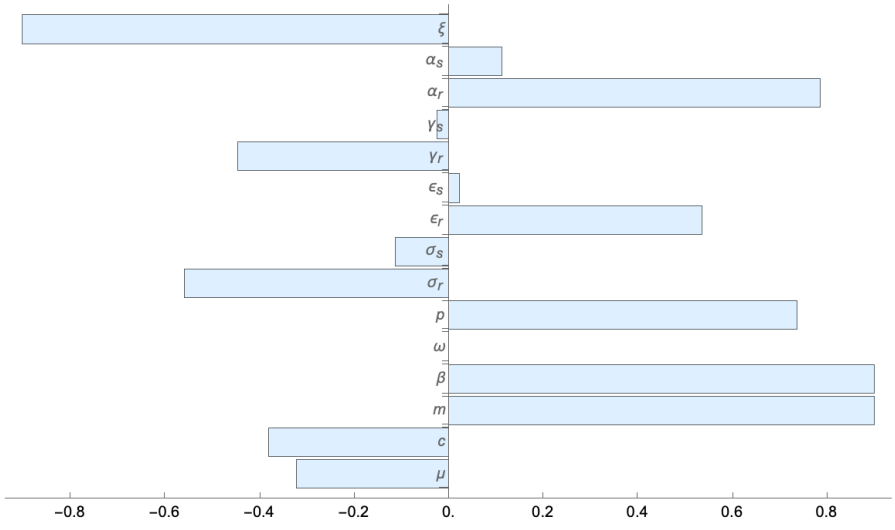

Figure 8. Sensitivity indices for basic reproduction number (R_0), with each sensitivity index corresponding to a model parameter.

Figure 8 illustrates the effects of varying each parameter value on the basic reproduction number (R_0). In this bar chart, we see how a slight increase in each parameter value will affect R_0 when the other parameters are kept at their default value. A positive sensitivity index indicates that increasing the parameter value will increase R_0, while negative sensitivity index

indicates that increasing the parameter value will decrease R_0. Given that a lower R_0 is better (R_0<1 indicates no endemic equilibrium), parameters with a negative sensitivity index should be increased to reduce the prevalence of malaria and parameters with a positive sensitivity index should be decreased to reduce the prevalence of malaria.

Given that the parameters for treatment rate and mosquito net use are negative, this figure supports the hypothesis that increasing these control measures will decrease the future prevalence of malaria in Nigeria. Given that the parameters for treatment failure rate are positive, this figure supports the hypothesis that decreasing treatment failure rates will decrease the future prevalence of malaria in Nigeria. The relative effects of varying these parameters is reflected in the magnitude of the sensitivity indices, where a larger magnitude corresponds to a larger change in R_0. Thus, this figure shows that increasing control measures for the resistant strain has a much more significant effect on reducing the prevalence of malaria than increasing control measures for the sensitive strain.

Figure 9

Original Results	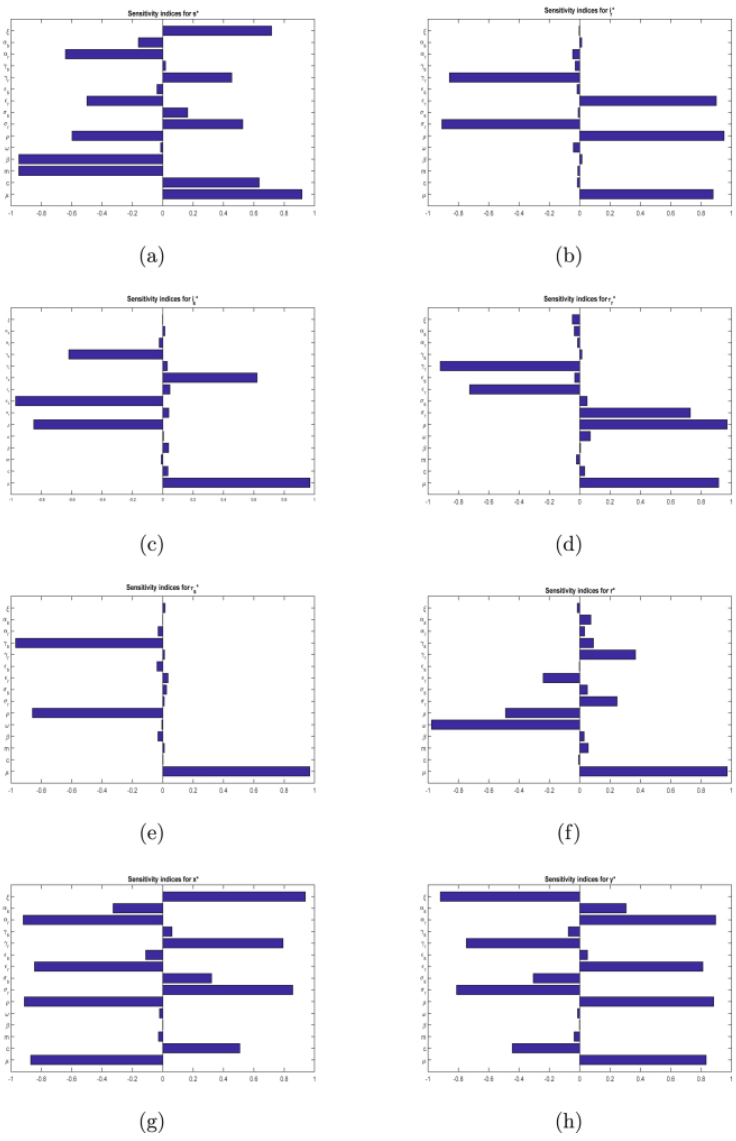

Figure 9. Tornado plot showing the sensitivity indices of the coexistence endemic equilibrium.

Our Results	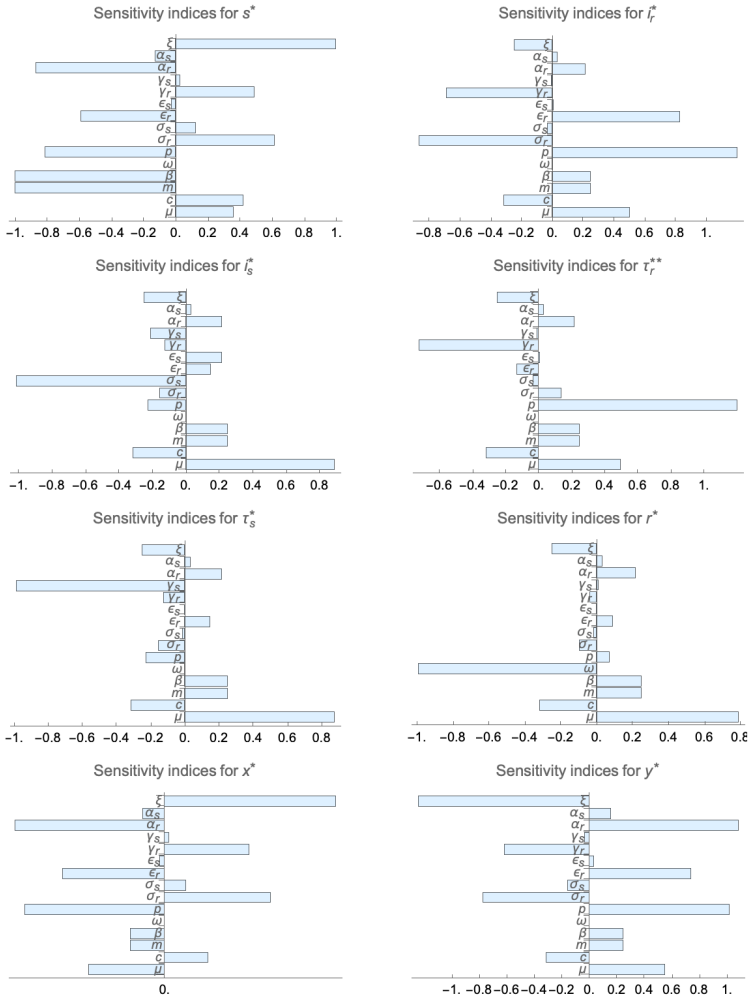

Figure 9. Sensitivity indices for the state variables of the coexistence endemic equilibrium, with each sensitivity index corresponding to a model parameter for each of the state variables.

Figure 9 illustrates the effect of varying each parameter value on the coexistence endemic equilibrium (CEE). In these bar charts, we see how a slight increase in each parameter value will affect the components of CEE when the other parameters are kept at their default value. A positive sensitivity index indicates that increasing the parameter value will decrease the CEE component, while negative sensitivity index indicates that increasing the parameter value will decrease the CEE component. Given that a lower CEE is better, parameters with a negative sensitivity index should be increased to reduce the prevalence of malaria and parameters with a positive sensitivity index should be decreased to reduce the prevalence of malaria.

Given that the the sensitivity indices for treatment rates (σ) and mosquito net use (c) are negative for i_r^* and i_s^*, this figure supports the hypothesis that increasing the treatment rate control measures will decrease the future prevalence of malaria in Nigeria. Given that the sensitivity indices for treatment failure rates (ϵ) are positive, this figure supports the hypothesis that decreasing the treatment failure rates will decrease the future prevalence of malaria in Nigeria.

Relation to Hypothesis

Figure 2 establishes Nigeria's historical malaria incidence data from 2000 to 2018. A model that cannot fit this historical data has little credibility as we know these values to be true. Figure 3 shows that the initial state variable and parameter values we use for the model produce a good fit for the model on historical data. This provides some confidence that the model can be used to predict the long-term dynamics of malaria accurately. Figure 4 shows the predicted long-term dynamics of malaria. This figure illustrates that 1) malaria will likely remain endemic in Nigeria until 2050 and 2) the resistant strain will dominate the outbreak. These points provide context for the control measure's reduction of malaria; malaria will continue to be an issue (particularly the resistant strain) without changes in control measures.

Figures 5, 6, and 7 directly show the effect of varying control measures on the long-term dynamics of malaria. Figure 5 illustrates that increasing the treatment rates of the sensitive/resistant strains decreases the prevalence of malaria, although not as well for the resistant strain. Figure 6 shows that reducing the treatment failure rates for the sensitive and resistant strains would reduce the prevalence of both malaria strains. Figure 7 shows that increasing the use of mosquito nets drastically decreases the prevalence of both strains by the year 2050. Thus, all of these control measure changes would help decrease the future prevalence of malaria in Nigeria and the hypothesis is affirmed.

Figures 8 and 9 illustrate the sensitivity indices for parameters as related to the basic reproduction number (R_0) and the coexistence endemic equilibrium (CEE). These sensitivity indices indicate how R_o and CEE will respond to changes in parameter values. Figure 8 indicates that increasing treatment rates and mosquito net use will decrease R_0, while decreasing treatment failure rates will decrease R_0. Figure 9 indicates that these changes will decrease i_r^* and i_s^* from CEE. Because lower values of R_0 and CEE indicate a lower future prevalence of malaria, these figures support the hypothesis that these changes will decrease future malaria prevalence in Nigeria.

Discrepancies

Figure 3

In Figure 3, our model estimate differs slightly from the authors' estimate between 2001 and 2002. This is most likely caused by differences in the initial values of x(t) and y(t), as we could not derive these values from the paper and thus fit them with Manipulate. However, this difference does not seem to propagate beyond 2002 in Figure 3 or affect Figure 4 at all (using the same model fit). The original Plot 3 (right) of Figure 4 does seem to have a sharp jump at t=0 years that our Figure 4 is missing. However, we believe this is an error in the original figure, as the proportion of susceptible humans (plot 1, left) is approximately 0.56 at t=0, which means the proportion of infected humans cannot be greater than 0.44 (the total normalized human population should be 1).

Figures 5 and 6

We struggled to exactly recreate Figures 5 and 6 from the information given in the paper. As mentioned in the results above, we believe the plot values represent the value of $i_s(t)$ or $i_r(t)$ at a specific value of t. Thus, the y-axis label should be $i_s(t)/i_r(t)$ instead of the original $i_s(t)$. This logic also aligns with how the authors describe the figure: "dynamics of infected humans with the resistant strain (dashed line) and the sensitive strain (solid line)" (Collins & Duffy, 2022). To attempt the replication, we created functions that get these values given a specific time, a parameter to change, and the new parameter value. First, we tried to develop each plot with the specific time of t=50 years. However, this only replicated the $i_s(t)$ plot correctly. We then used Manipulate to find the time (between 0 and 100 years) that would reproduce the figures as closely as possible. We found the following specific times replicated the plots the best: t=22 years for Figure 5 $i_r(t)$, t=19 years for Figure 6 $i_r(t)$, t=41 years for Figure 6 $i_s(t)$. Although Figure 5 is reproduced very well, the $i_r(t)$ plot of Figure 6 is still slightly off. This discrepancy may result from our fit values for x_0 and y_0 being different from the values used in the paper.

Figures 8 and 9

We struggled to exactly recreate Figures 8 and 9. Although Figure 8 is nearly identically reproduced, some sensitivity indices still vary between the original and replicated figures. For example, the sensitivity index for α_s in the original figure is slightly above 0.2 while in the

replicated figure this sensitivity index is slightly below 0.2. For the most part, the original and replicated figures have the same relative magnitudes and signs for each sensitivity index with the exception of ω. In the original figure, the sensitivity index for ω is slightly below 0 while in the replicated figure it is exactly 0.

Figure 9 has more significant differences between the original and replicated versions. In this figure, some of the relative magnitudes and signs of the sensitivity indices differ significantly between the original and replicated figures. For example, for the sensitivity index of α_r for i_s^* in the original figure is slightly below 0 while in the replicated figure it is slightly above 0.2. These sign differences can be seen throughout the components of the coexistence endemic equilibrium, except for s^* which seems to have all the same sensitivity index signs for its original and replicated versions.

The differences we observe between these original and replicated versions of these two figures is likely a result of our approach to creating the figures. In the original paper, Collins and Duffy (2022) say “the Latin Hypercube Sampling Method (LHSM) is considered for the sensitivity analysis. From the LHSM, the partial rank correlation coefficients (PRCCs) of R_0 and the coexistence endemic equilibrium are calculated”. They then plotted the “sensitivity effects (based on the PRCC values)” for each parameter to create Figures 8 and 9. Given our knowledge and time constraints, we were unable to replicate the use of LHSM and PRCCs to derive the sensitivity indices. We instead calculate the normalized forward sensitivity indices as described by Samui et al., (2020) and implemented in Mathematica by Gareth Russell of the New Jersey Institute of Technology in this Wolfram Community forum post (2022): https://community.wolfram.com/groups/-/m/t/2719372. This different method of calculating the sensitivity indices likely resulted in the differences seen between the original and replicated figures.

Extension

Because we could not find literature values for the parasite reduction (pr) and spread constant (sc), we chose to first see how arbitrary pr and sc values of 0.9 and 0.05 affect the predicted incidence of malaria in Nigeria. As a reminder, the reduction factor is only implemented after 2025 to model the release of these genetically modified mosquitoes at this time. Incorporating a reduction factor with these arbitrary pr and sc values after 2025 (when the malaria-stunting gene could realistically be used across Nigeria) produces the following i_r and i_s plots:

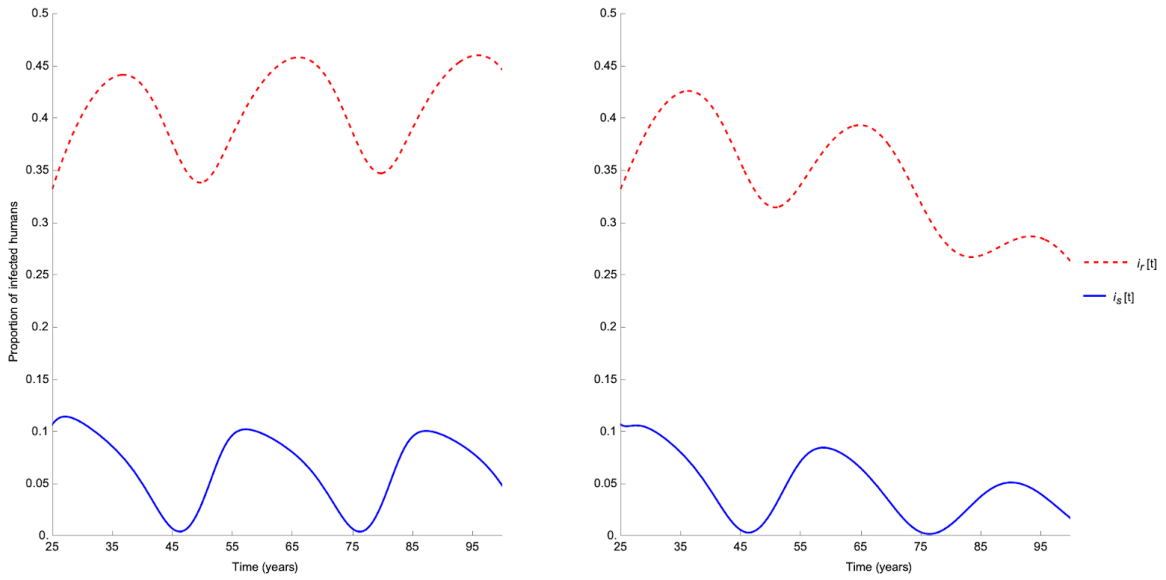

Extension Figure 1. Malaria dynamics in Nigeria as predicted by model without reduction factor (left) and with reduction factor (right) during 2025 to 2100.

Clearly, the reduction factor modeling the spread of the malaria-resistant gene through the population helps reduce malaria prevalence. The model without the reduction factor (left) indicates that malaria, particularly the resistant strain, will remain endemic to Nigeria from 2025 to 2100, varying with the seasonality factor of the transmission rate. However, with the reduction factor the overall future malaria prevalence significantly decreases as the malaria-stunting gene spreads through the population. To see how i_r and i_s values would differ with pr and sc values, we create contour plots for these infected human population values at time t = 100 (2100) across all pr and sc values.

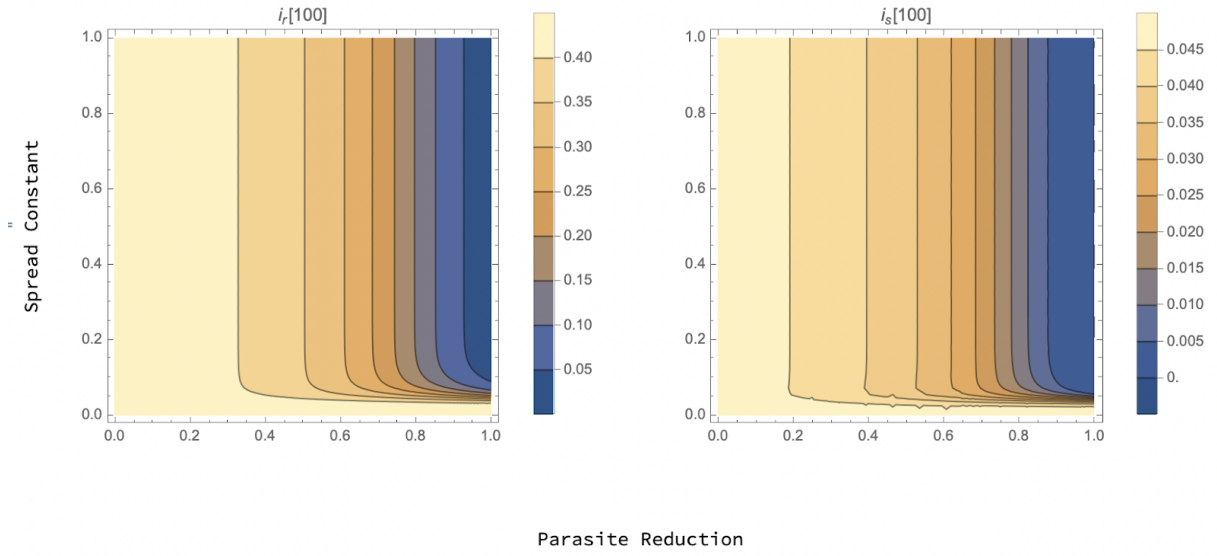

Extension Figure 2. i_r and i_s values at t = 100 (year 2100) for various values of parasite reduction and spread constant.

This figure demonstrates which parasite reduction and spread constant values best reduce the resistant and sensitive strain prevalence at 2100. In a biological context, this figure gives context to what scientists should focus on when developing this gene drive method. For example, to achieve a resistant-strain incidence of less than 0.05 by 2100, a malaria-stunting gene must have an efficacy of over 95% and a spread constant of more than 0.15. These results also show that after a specific parasite reduction value (0.4), improving the spread constant is significantly more valuable in decreasing future malaria prevalence and vice versa.

When considering a malaria-stunting gene as a control measure for the disease, both of these figures support the hypothesis that increasing control measures for malaria will decrease the future prevalence of malaria. Extension Figure 1 illustrates that for the arbitrary pr and sc values of 0.9 and 0.05, malaria incidence at t=100 years (2100) decreases from about 0.45 to 0.25 and 0.05 to 0.02 for the resistant and sensitive strains, respectively. Extension Figure 2 illustrates that any sc and pr values above 0.1 and 0.4 will decrease the prevalence of malaria at 2100 for both the resistant and sensitive strains. Furthermore, the extended model predicts that a combination of sc and pr values above 0.1 and 0.9 would nearly eradicate both strains of malaria in Nigeria by 2100.

Discussion

Hypothesis Analysis

Again, the paper hypothesizes that a model can be used to indicate that the prevalence of malaria in Nigeria will decrease if control measures, particularly improved treatment and increased mosquito net usage, are improved and made widespread.

Three sets of dimensionless parameters (referred to as control measures) play a significant role in the dynamics of malaria observed in this paper. The first set of parameters is treatment rates (one for both the resistant and sensitive strains), which is used to quantify the rate at which humans infected with malaria are treated. This treatment either succeeds and the person becomes temporarily immune, or the treatment fails, and the person dies. The next set of parameters is treatment failures (one for both the resistant and sensitive strains), which is used to quantify the chance that a treated human dies due to the disease. The final control measure is the use of mosquito nets, which is used to quantify the use of mosquito nets and the

subsequent reduction of infection. The analyses undertaken in the original paper and our recreation sought to understand how these three control measures could be used to predict the dynamics of malaria in Nigeria. Two normalized populations, humans infected with the resistant strain (i_r) and humans infected with the sensitive strain (i_s), were studied to learn how these populations vary as the control parameters change. Of these systems studied, i_r and i_s were both found to be responsive to changes in treatment failure and mosquito net use. Both systems decreased to nearly 0 as treatment failures decreased and mosquito net use increased. While i_s was found to decrease to nearly 0 with increased treatment rates, i_r did not decrease nearly as much. Thus, the model indicates that malaria's prevalence in Nigeria will decrease if treatment failure is reduced and mosquito net use is more widespread. Although the model also indicates the prevalence of malaria will decrease if treatment rates are improved, the resistant strain will likely still remain pervasive with these increased treatment rates. Overall, the model mostly supports the hypothesis that improved control measures will decrease the prevalence of malaria.

Other scientific literature does not not support the assumptions of the model very well. The first assumption of the model is that all humans can be put into one of 6 categories: susceptible, infected (resistant), infected (sensitive), treated (resistant), treated (sensitive), and recovered/immune. However, other research suggests humans should also be able to be classified into a latent class (Ndamuzi & Gahungu, 2021). This latent class would include humans that have been exposed to malaria and have contracted the parasite but are not yet able to infect mosquitoes as the parasite grows. Thus, the first assumption of this model is incorrect as it does not include the latent category of humans for the sensitive or resistant strain. Similarly, the second assumption of this model does not match data in the literature. This second assumption is that all mosquitoes can be categorized as susceptible or infected. However, Howick et al. (2019) explain that the malaria parasite undergoes development in a mosquito before becoming infectious to humans. Thus, some mosquitoes should also be able to be categorized into a latent category and the second assumption of the model is incorrect. The third assumption of this model is that the birth and death rates of the mosquito and human populations are the same, thus these total populations remain constant. Nguyen et al. (2021) show that the annual population growth of each Nigerian state is greater than 0% from 2006 to 2016, with a national average population growth of 3.93% during this time period. Okorie et al. (2014) demonstrate that the abundance of mosquitoes in Ibadan, Southwestern Nigeria varies significantly with the rainfall, temperature, and relative humidity. It is not unreasonable to extrapolate this data to all of Nigeria and conclude that total mosquito population does not

remain constant but instead varies with the aforementioned factors. Thus, the model's assumption that human and mosquito populations remain constant is not supported at all by literature. The final assumption of this model is that humans recovering from malaria have temporary immunity from reinfection. That is, after someone has been infected with malaria and has recovered they are 100% immune from infection for a period of time. This does seem to fit with previous research that indicates naturally acquired malaria immunity should be appreciated as nearly 100% effective against severe disease for heavily exposed adults and more than 90% effective for exposed infants (Doolan et al., 2009). Thus, only the final assumption of the model that those who recently recovered from a malaria infection are immune for some time is supported by data in the literature. The data in the literature do not support the other four assumptions of the model.

Recreation Discrepancies

My partner and I attempted to recreate all figures from the original paper using the differential model for malaria dynamics. Although we could replicate most of the figures, we struggled to interpret how some were created and replicate these ourselves. We were initially unable to create Figure 2 as the World Bank (2021) page cited by the original authors had been updated to reflect different malaria incidence data. However, the original authors kindly provided this data via email after we reached out to them. We also struggled to replicate Figure 3 due to a typo in Table 3 that makes it seem like the m parameter has a variable value. After we reached out, the authors clarified that this parameter had a constant value and shared this value with us. We then used Manipulate to find the x(0) and y(0) initial state variable values that best recreated Figure 3. Our version of Figure 3 differs slightly from the original for 2000-2002. However, this discrepancy does not affect our conclusions about the biological system because it did not affect the model fit after 2002. This perfect fit after 2002 is demonstrated by the perfect match of Figure 3 after 2002 and the perfect match of our Figure 4 with the original Figure 4.

We struggled to perfectly reproduce Figures 5 and 6 given the information in the paper (see Results). Although we were able to replicate Figure 5 nearly perfectly, the $i_r(t)$ plot of our Figure 6 seems to consistently be about 0.05 above the original Figure 6. This discrepancy would affect our conclusions about the biological system by suggesting that decreasing the resistant treatment failure parameter value does not reduce the incidence of malaria as much as the original paper suggests. However, this minor discrepancy does not change the overall conclusion drawn from Figure 6 – decreasing the resistant treatment failure parameter value greatly reduces the malaria incidence.

We were unable to exactly replicate Figure 8 given the information provided in the paper and our knowledge/time constraints. The discrepancies in Figures 8 were mostly related to the magnitude of the sensitivity indices. No sensitivity indices had differing signs in the original and replicated versions except ω, which changed from a slightly negative number to 0. However, these magnitude and sign differences did not affect our conclusions about the biological system. The signs of the control-measure related parameters (treatment rates, treatment failure rates, and mosquito net use) in both versions of the figure support the conclusion that increasing treatment rates/mosquito net use and decreasing treatment failure rates will decrease future malaria prevalence in Nigeria. Furthermore, the relative magnitudes of these sensitivity indices for both versions of the figure indicate that adjusting the parameters related to the resistant strain can reduce the future malaria incidence much more than adjusting the parameters related to the sensitive strain.

Similarly to Figure 8, we were unable to exactly replicate Figure 9 given the information provided in the paper and our knowledge/time constraints. However, for this figure there are some differences for the signs and magnitudes of the sensitivity indices between the original and replicated figures. The only sensitivity index parameters we focused on for analysis were related to control measures (treatment rates, treatment failure rates, and mosquito net use), and these all had the same signs between the original and replicated figures for i_r^* and i_s^*. Thus, this difference does not drastically affect our conclusions about the biological system. However, anyone using Figure 9 for analysis might differ in their understanding of how a parameter change would affect the coexistence endemic equilibrium (CEE) depending on which version of the figure they are using for analysis. Any sensitivity index that changes in sign between the two figures would reflect a change in how the CEE would be affected by a change in that parameter.

Limitations

While the model for malaria dynamics studied by Collins and Duffy has produced meaningful results that can be applied to predict the future dynamics of malaria in Nigeria, it is subject to severe simplifications that limit its ability to be applied to the real world. Many of the model's simplifications are a result of its underlying assumptions. As discussed in hypothesis analysis, only the final assumption that humans recently recovered from malaria are immune to reinfection for some time is supported by other literature. The rest of the assumptions help make the model simpler and work to fit historical data but likely cause the model to become inaccurate

for future malaria dynamics predictions, especially for the distant future. Thus, using this model for long-term dynamics predictions may be a bad idea.

This model also makes other simplifications that could limit its applicability. For example, this model assumes that there are only two strains of malaria - resistant to treatment and sensitive to treatment. However, research suggests that at least six species of malaria parasites are part of the mosquito-human life cycle. Each of these six malaria species can then develop resistance or maintain their sensitivity to antimalarial drugs (Milner, 2018). The different strains of each of these species would then have different treatment failure rates and rates of infection. Thus, assuming there are only two strains of one malaria species, as is done in this model, is quite a simplification that could limit the accuracy of this model's predictions. Its broad geographic area of focus also limits this model. Previous research has demonstrated that malaria dynamics can vary with geographic loci (Wellems & Plowe, 2001), as malaria dynamics can be affected by the conditions of the geographic loci and the people living there. Thus, attempting to model the dynamics of malaria in a region as large as Nigeria is likely far less accurate than modeling the dynamics of malaria in a smaller region like a state. While these limitations are relevant to the model's accuracy, especially for distant future predictions, they do not necessarily detract from the significance of the results obtained by Collins and Duffy. These results still likely show some significant relationship between the control measures analyzed and the resulting changes in malaria dynamics in Nigeria.

Comparison to Other Models

After recognizing the limitations of the model created by Collins and Duffy, we searched for other models of disease that had overcome some of the simplifications made by this model. Ndamuzi and Gahungu (2021) have created a malaria model for Burundi (East Africa) that incorporates the latent category for humans that have contracted the malaria parasite but do not yet have symptoms (and thus are not being treated) and are unable to transmit the parasite to mosquitoes. While the authors could fit this model to real data, the fit is quite bad. Also, the authors choose not to include a latent category for mosquitoes that have contracted the parasite but cannot yet infect humans. Thus, this paper could not successfully include a latent category in their state variables for malaria analysis.

Future Work

In the future, we hope to find literature values for the parameters and state variable initial values of the model that had to be fit to historical data (c, σ_r, σ_s, ϵ_r, ϵ_s, x(0), and y(0)). This would help us better understand how the model would perform conditions as close to reality. Finding literature values for the parasite reduction and spread constant used in the extension would also ensure that the model is as realistic as possible. We also aim to overcome the simplicities of our model by no longer using the incorrect assumptions stated in the original paper (see hypothesis analysis). This final model would include state variables for latent humans and mosquitoes (in addition to those already included), which Sattenspiel (1990) mentions can improve the model's accuracy when implemented correctly. Incorporating a variable total human and mosquito population could also help improve the reliability of this model (Liu & Driessche, 1995).

Extension

Our extension expands the hypothesis to include a maria-stunting gene as a control measure. While we do now know the real values for parasite reduction and spread constant (we could not find these in the literature), we show in Figure 2 which combinations of these values will produce reduced incidence of malaria at t=100 (2100) for both strains. Figure 2 demonstrates the effect of introducing a maria-reducing gene on the prevalence of both strains over time. Clearly, these extension results show that improving this control measure will reduce the future prevalence of malaria in Nigeria. While our extension can provide some insight into the dynamics of malaria as a malaria-stunting gene spreads through a mosquito population, it is limited by its long-term analysis and simplicity. Our model can fit historical data very well, but the further we deviate from this historical data, the less accurate we can expect our model's predictions to be. Thus, attempting to predict malaria incidence out as far as 2100, which is done in both figures, will likely not be very accurate.

Furthermore, this extended model likely oversimplifies the complexities of gene transmission. For example, Buchman et al. (2018) demonstrate that for some cases of Madea gene drive (the gene drive system we consider in the extension), a population can develop "drive resistance" that reduces the spread of the desired gene. Incorporating these complexities into a future version of this extended model would help overcome these simplicities and their resulting model limitations.

References

1. Collins, O. C., & Duffy, K. J. (2022). A mathematical model for the dynamics and control of malaria in Nigeria. *Infectious Disease Modelling*, 7(4), 728–741. https://doi.org/10.1016/j.idm.2022.10.005

2. Olumuyiwa James Peter, Mayowa M. Ojo, Ratchada Viriyapong & Festus Abiodun Oguntolu (2022) Mathematical model of measles transmission dynamics using real data from Nigeria, *Journal of Difference Equations and Applications*, 28:6, 753-770. https://doi.org/10.1080/10236198.2022.2079411

3. Kumar, H., Arora, P. K., Pant, M., Kumar, A., & Akhtar Khan, S. (2021). A simple mathematical model to predict and validate the spread of Covid-19 in India. *Materials today*. Proceedings, 47, 3859–3864. https://doi.org/10.1016/j.matpr.2021.03.434

4. Fatmawati, & Tasman, H. (2015). An optimal control strategy to reduce the spread of malaria resistance. *Mathematical biosciences*, 262, 73–79. https://doi.org/10.1016/j.mbs.2014.12.005

5. Basu, S., & Sahi, P. K. (2017). Malaria: An Update. *Indian journal of pediatrics*, 84(7), 521–528. https://doi.org/10.1007/s12098-017-2332-2

6. Lalloo, D. G., Shingadia, D., Bell, D. J., Beeching, N. J., Whitty, C. J. M., Chiodini, P. L., & PHE Advisory Committee on Malaria Prevention in UK Travellers (2016). UK malaria treatment guidelines 2016. *The Journal of infection*, 72(6), 635–649. https://doi.org/10.1016/j.jinf.2016.02.001

7. *The World Bank*. (2021). World Bank Open Data. Retrieved April 18, 2023, from https://data.worldbank.org/indicator/SH.MLR.INCD.P3?end=2021&locations=NGk-NG&start=2000&view=chart

8. Samui, P., Mondal, J., & Khajanchi, S. (2020). A mathematical model for COVID-19 transmission dynamics with a case study of India. *Chaos, solitons, and fractals*, *140*, 110173. https://doi.org/10.1016/j.chaos.2020.110173

9. Nguyen, P. Y., Ajisegiri, W. S., Costantino, V., Chughtai, A. A., & MacIntyre, C. R. (2021). Reemergence of Human Monkeypox and Declining Population Immunity in the Context of

Urbanization, Nigeria, 2017-2020. *Emerging infectious diseases*, *27*(4), 1007–1014. https://doi.org/10.3201/eid2704.203569

10. Okorie, P. N., Popoola, K. O., Awobifa, O. M., Ibrahim, K. T., & Ademowo, G. O. (2014). Species composition and temporal distribution of mosquito populations in Ibadan, Southwestern Nigeria. *Journal of entomology and zoology studies*, *2*(4), 164–169.

11. Doolan, D. L., Dobaño, C., & Baird, J. K. (2009). Acquired immunity to malaria. *Clinical microbiology reviews*, *22*(1), 13–36. https://doi.org/10.1128/CMR.00025-08

12. Wellems, T. E., & Plowe, C. V. (2001). Chloroquine-resistant malaria. *The Journal of infectious diseases*, *184*(6), 770–776. https://doi.org/10.1086/322858

13. Milner D. A., Jr (2018). Malaria Pathogenesis. *Cold Spring Harbor perspectives in medicine*, *8*(1), a025569. https://doi.org/10.1101/cshperspect.a025569

14. Ndamuzi, E. and Gahungu, P. (2021) Mathematical Modeling of Malaria Transmission Dynamics: Case of Burundi. *Journal of Applied Mathematics and Physics*, 9, 2447-2460. doi: 10.4236/jamp.2021.910156.

15. Howick, V. M., Russell, A. J. C., Andrews, T., Heaton, H., Reid, A. J., Natarajan, K., Butungi, H., Metcalf, T., Verzier, L. H., Rayner, J. C., Berriman, M., Herren, J. K., Billker, O., Hemberg, M., Talman, A. M., & Lawniczak, M. K. N. (2019). The Malaria Cell Atlas: Single parasite transcriptomes across the complete *Plasmodium* life cycle. *Science (New York, N.Y.)*, *365*(6455), eaaw2619. https://doi.org/10.1126/science.aaw2619

16. Pascini, T. V., Jeong, Y. J., Huang, W., Pala, Z. R., Sá, J. M., Wells, M. B., Kizito, C., Sweeney, B., Alves E Silva, T. L., Andrew, D. J., Jacobs-Lorena, M., & Vega-Rodríguez, J. (2022). Transgenic Anopheles mosquitoes expressing human PAI-1 impair malaria transmission. *Nature communications*, *13*(1), 2949. https://doi.org/10.1038/s41467-022-30606-y

17. Marshall, J. M., & Taylor, C. E. (2009). Malaria control with transgenic mosquitoes. *PLoS medicine*, *6*(2), e20. https://doi.org/10.1371/journal.pmed.1000020

18. Wade, M. J., & Beeman, R. W. (1994). The population dynamics of maternal-effect selfish genes. *Genetics*, *138*(4), 1309–1314. https://doi.org/10.1093/genetics/138.4.1309

19. Collins, J., & Abdelal, N. (2018). Spread of Disease. *AMSI Calculate*, https://calculate.org.au/wp-content/uploads/sites/15/2018/10/spread-of-disease.pdf

20. Sattenspeil, L. (1990). Modeling the Spread of Infectious Disease in Human Populations. *Yearbook of Physical Anthropology*, 133:245-276. https://doi.org/10.1002/ajpa.1330330511

21. Liu, W.M., & Driessche, P. (1995). Epidemiological models with varying population size and dose-dependent latent period. *Mathematical Biosciences, 128*(1), 57-59. https://doi.org/10.1016/0025-5564(94)00067-A

22. Buchman, A., Marshall, J. M., Ostrovski, D., Yang, T., & Akbari, O. S. (2018). Synthetically engineered *Medea* gene drive system in the worldwide crop pest *Drosophila suzukii*. *Proceedings of the National Academy of Sciences of the United States of America*, *115*(18), 4725–4730. https://doi.org/10.1073/pnas.1713139115